Evidence for a Population of Sleepy Sodium Channels in Squid Axon at Low Temperature

DONALD R. MATTESON and CLAY M. ARMSTRONG

From the Department of Physiology, University of Pennsylvania School of Medicine, Philadelphia, Pennsylvania 19104; and The Marine Biological Laboratory, Woods Hole, Massachusetts 02543

ABSTRACT We have studied the effects of temperature changes on Na currents in squid giant axons. Decreases in temperature in the 15–1°C range decrease peak Na current with a Q_{10} of 2.2. Steady state currents, which are tetrodotoxin sensitive and have the same reversal potential as peak currents, are almost unaffected by temperature changes. After removal of inactivation by pronase treatment, steady state current amplitude has a Q_{10} of 2.3. Na currents generated at large positive voltages sometimes exhibit a biphasic activation pattern. The first phase activates rapidly and partially inactivates and is followed by a secondary slow current increase that lasts several milliseconds. Peak Na current amplitude can be increased by delivering large positive prepulses, an effect that is more pronounced at low temperatures. The slow activation phase is eliminated after a positive prepulse. These results are consistent with the hypothesis that there are two forms of the Na channel: (*a*) rapidly activating channels that completely inactivate, and (*b*) slowly activating "sleepy" channels that inactivate slowly if at all. Some fast channels are assumed to be converted to sleepy channels by cooling, possibly because of a phase transition in the membrane. The existence of sleepy channels complicates the determination of the Q_{10} of gating parameters and single-channel conductance.

INTRODUCTION

Several recent studies have shown that the phospholipid phase of biological membranes can undergo a transition to a more ordered structure as the temperature is lowered (Chapman, 1975). A phase transition in biological systems is evidenced by a change in activation energy at the transition temperature (Kumamoto et al., 1971), and this change can be demonstrated as an alteration in the slope of an Arrhenius plot. For example, Schwarz (1979) has shown that Arrhenius plots of the Hodgkin and Huxley (1952) parameters τ_m and τ_h, calculated from Na currents recorded from frog skeletal muscle, exhibit a change in slope between 5 and 8°C, which indicates that the

Address reprint requests to Dr. Donald R. Matteson, Dept. of Physiology, University of Pennsylvania School of Medicine, Philadelphia, PA 19104.

J. GEN. PHYSIOL. © The Rockefeller University Press · 0022-1295/82/05/0739/20 $1.00 739
Volume 79 May 1982 739–758

membrane lipid or the channel protein itself has undergone a phase transition. Similar results were reported for squid giant axons by Kimura and Meves (1979) and for node of Ranvier by Chiu et al. (1979). We have studied the influence of temperature on the sodium channel in squid giant axons and our results are consistent with the hypothesis that a decrease in temperature transforms some normal sodium channels into slowly activating, noninactivating "sleepy" channels. Channel transformation, we speculate, may be the result of a phase transition in the membrane lipids over the temperature range roughly from 10 to 1°C. C. Sevcik (personal communication), using methods different from ours, has also come to the conclusion that there is a population of slowly activating Na channels in intact squid axons. A slow sodium current has also been demonstrated in cerebellar Purkinje fibers (Llinas and Sugimori, 1980).

Recent results have introduced some uncertainty regarding the commonly accepted value of the Q_{10} of sodium permeability magnitude, $\bar{P}_{Na}$ or $\bar{g}_{Na}$. Kimura and Meves (1979) found that peak I_{Na} had a Q_{10} of 1.9–3.9 (0–10°C). In terms of Hodgkin and Huxley's model, this corresponded to a Q_{10} for $\bar{P}_{Na}$ of 2.9–6.0. Chandler and Meves (1970*b*) had previously reported a Q_{10} of 1.6 for $\bar{g}_{Na}$ in the squid, whereas Frankenhaeuser and Moore (1963) found a value of 1.3 for the node of Ranvier, and Schauf (1973) noted a value of 1.3 for *Myxicola* giant axons. The Q_{10} of $\bar{P}_{Na}$ (or $\bar{g}_{Na}$) is of interest because it is related to the height of the energy barriers encountered by a Na ion traversing the membrane field. We find a Q_{10} for peak Na current of 2.2, which is in reasonable agreement with the range of 1.9–3.9 reported by Kimura and Meves (1979) for this same parameter. This relatively high Q_{10} could be due to lower single-channel conductance at lower temperatures, which is the usual hypothesis, or to fewer channels opening at low temperature. If, as suggested above, there are functionally two populations of channels, and the fraction that activates slowly increases as temperature is lowered, fewer channels will be conducting at the peak of the Na current. By applying our model, which assumes two channel types, we obtain a Q_{10} of 1.8 for $\bar{P}_{Na}$ or $\bar{g}_{Na}$, which is significantly less than the values reported by Kimura and Meves; this indicates that these Q_{10} determinations are model dependent. Preliminary accounts of this work have appeared elsewhere (Matteson and Armstrong, 1980*a* and *b*).

METHODS

Experiments were performed on segments of isolated giant axons of *Loligo pealii*, obtained at the Marine Biological Laboratory, Woods Hole, MA. Axons were cleaned of all adhering fibers and internally perfused. The techniques used here were the same as those described previously (Bezanilla and Armstrong, 1977; Armstrong and Gilly, 1979). The linear portion of the currents was subtracted using the P/4 method (Armstrong and Bezanilla, 1974).

Temperature was sensed by a small thermistor mounted in the floor of the chamber, approximately midway between the left- and right-hand walls. Thermistor resistance constituted the input to a negative feedback controller that regulated temperature with a Peltier device. The Peltier was in thermal contact with a silver block that also served as guard electrodes for the rear section of the chamber. External solution

flowing into the chamber was precooled by the same Peltier. Temperature control under these conditions might be imperfect because of slight temperature gradients from the rear to the front of the chamber. Such gradients could produce multiple kinetic components in ionic currents, but it is extremely unlikely that any such gradients would be large enough to explain the highly disparate kinetic components reported in this paper. In support of this notion, we have recently modified our chamber so that its floor is constructed of silver that is in contact with the Peltier so as to minimize temperature gradients. Results obtained with the modified chamber agree completely with our previous results. After a temperature change we waited 2–3 min for thermal equilibration before continuing with the experiment.

The names and compositions of all solutions used in this study are listed in Table I. The solutions are referred to as external solution//internal solution.

The influence of temperature on certain parameters of Na channel behavior is characterized by the temperature coefficient (Q_{10}) of the effect. Approximate Q_{10}'s were calculated according to the equation

$$Q_{10} = (k_2/k_1)^{10/(T_2 - T_1)}$$

where k_2 is the value of the parameters obtained at the higher temperature (T_2) and k_1 is the value at the lower temperature.

TABLE I
SOLUTIONS

External solutions (mM)	Trizma 7.0*	NaCl	$CaCl_2$
ASW	—	450	50
1/4 Na	360	113	50
Tris TTX‡	480	—	50

Internal Solutions (mM)§	K	TMA	F	Glutamate	Sucrose
275 KFG	275	—	50	225	420
200 TMA	—	200	50	150	560

* Tris (hydroxymethyl) aminomethane (Sigma Chemical Co., St. Louis, MO).
‡ Tetrodotoxin, 200 nM.
§ Internal solutions were buffered with 10 mM Trizma 7.0.

RESULTS

Peak and Steady State I_{Na} vs. Temperature

The major effects of temperature changes on Na current amplitudes are illustrated in Fig. 1: peak amplitude decreases as the temperature is lowered, but steady state currents are relatively unaffected. For the two fibers illustrated in Fig. 1, as well as all others reported in this paper, K currents have been abolished by removing K ions from both sides of the membrane. The Na currents shown were generated by voltage-clamp steps to +20 mV (A) and +40 mV (B) for a duration of 36 ms at each of the indicated temperatures. The maintained current level evident at the end of the voltage-clamp steps can be identified as Na current because it is blocked by tetrodotoxin (TTX) and it has the same reversal potential as peak currents (see also Chandler and Meves, 1970*a*). For the two axons illustrated, the peak amplitude of the Na

current decreased substantially as the temperature was reduced. The Q_{10} of this effect was 2.24 for the axon shown in Fig. 1A and 2.66 for that shown in Fig. 1B. The mean Q_{10} of peak I_{Na} was 2.24 ± 0.29 for six fibers studied (see Table II). This figure is in reasonable agreement with the Q_{10} range of 1.9–3.9 reported by Kimura and Meves (1979) in the 0–10°C range.

The effect of temperature on steady state Na current is quite different from the effect on peak current. The current level at the end of a 36-ms voltage-clamp step is sometimes changed very little (Fig. 1A) or, in other cases, it

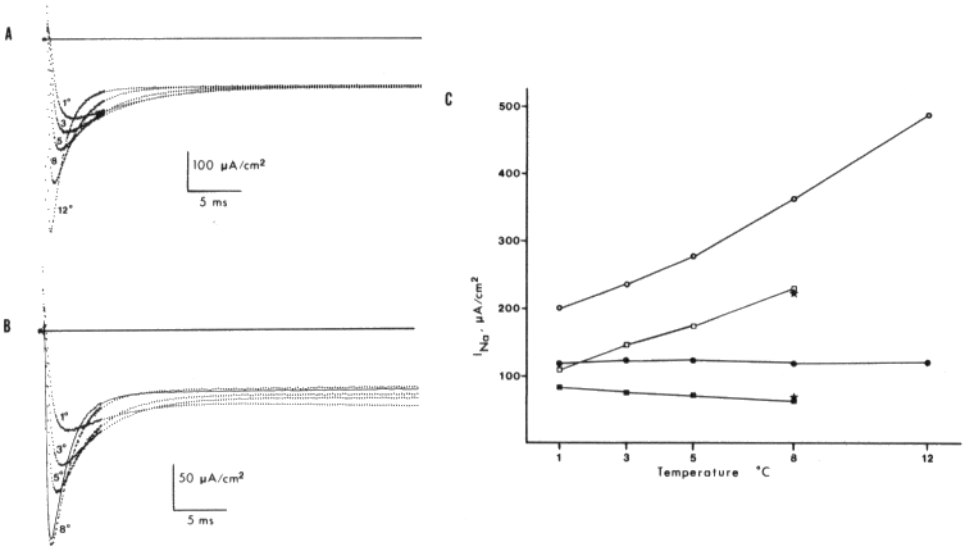

FIGURE 1. (A) Na currents recorded during steps to +20 mV at each of the indicated temperatures. The records were obtained in the following order: 8, 5, 3, 1, 12°C. Axon AU109B. The holding potential was −80 mV. 1/4 Na//200 TMA. (B) Na currents recorded during steps to +40 mV at each of the indicated temperatures. Temperature was changed in the following order: 8, 5, 3, 1°C. The solid trace was obtained upon returning the temperature to 8°C after the above sequence. Axon AU119A. The holding potential was −80 mV. 1/4 Na/ /200 TMA. (C) Current vs. temperature relationships for the records shown in A (plotted with circles) and B (plotted as squares). Open symbols show peak current and filled symbols show steady state current. The stars, which plot currents from B recorded after return to 8°C, indicate reversibility of the temperature effect.

actually increases in magnitude as the temperature is lowered (Fig. 1B). The increase in steady state current illustrated in Fig. 1B is a reversible effect, as shown by the recovery of the control current level upon return of the preparation to 8°C.

The peak and steady state current magnitudes are plotted as a function of temperature in Fig. 1C and the differential effect of temperature on these Na currents is apparent. The differential effect might be explained by assuming

that single-channel conductance is unaffected by temperature and that as the temperature is lowered fewer channels contribute to peak current but the number of channels conducting in the steady state is constant. To test this explanation we examined Na currents at various temperatures in the absence of inactivation. After inactivation was removed by perfusion with pronase (Armstrong et al., 1973), the steady state Na current level decreased as the temperature was lowered from 8 to 1.4°C, as shown in Fig. 2. The Q_{10} of the effect was 2.30, which is comparable to the Q_{10} of the peak amplitude decrease in the presence of inactivation. Because gating current experiments have suggested that the size of the Na channel population is relatively temperature insensitive (Bezanilla and Taylor, 1978), this result suggests that single Na channel conductance has a Q_{10} of ~2.3. In a nonpronased axon, if single-channel conductance during the peak and steady state are equally affected by temperature changes, there must be more channels conducting in the steady state at lower temperatures.

Another interesting feature of the Na currents shown in Fig. 2 is their

TABLE II

Q_{10} OF PEAK CURRENT

Experiment	Temperature range	Q_{10}
	°C	
JN199B	1.5–15	2.09
JN229B	3–15	1.84
AU109B	1–12	2.24
AU119A	1–8	2.66
AU229B	1–12	2.14
AU259A	1–8	2.44
	Mean ± SD	2.24±0.29

apparent biphasic activation pattern. The initial rapid activation phase is followed by a slow increase in current that has a time constant of ~10 ms at 1.4°C. Although the slow phase of current increase is more visible in the absence of inactivation, we sometimes observe the same phenomenon in nonpronased axons, where it is generally more noticeable at low temperatures and at positive voltages. The Na currents shown in Fig. 3 were generated by voltage-clamp steps to +60 mV at the indicated temperatures. At 8°C the Na current activates and then inactivates to a sustained nonzero level, which remains more or less constant throughout the 36-ms pulse. However, at 1°C the record shows an additional slow increase in current after inactivation. This slow activation phase is a reversible effect of temperature, as shown by the current recorded upon return of the preparation to 8°C (solid trace in Fig. 3). The slow current increase might conceivably be generated by one of the following mechanisms: (*a*) inactivated channels might be reopening through a transition to the h_2 state of Chandler and Meves (1970*a*), or (*b*) a population of Na channels may exist that activates very slowly. We believe that the experiments to be described below support the second mechanism.

Na Current Potentiation by Prepulses

While examining the influence of temperature on the rate of recovery from inactivation, we found that large positive prepulses could increase the peak Na current generated by a test pulse delivered ~20 ms after the prepulse. The pulse protocol for this experiment is shown in the inset of Fig. 4A. The first pulse (to +90 mV) was used to inactivate the Na conductance. The second pulse, to −10 mV, was separated from the first by a variable interval and used to assess the amount of Na current that had recovered from the preceding depolarization. In Fig. 4 the peak amplitude of the Na current generated by the second pulse is plotted as a function of the interval between pulses. The

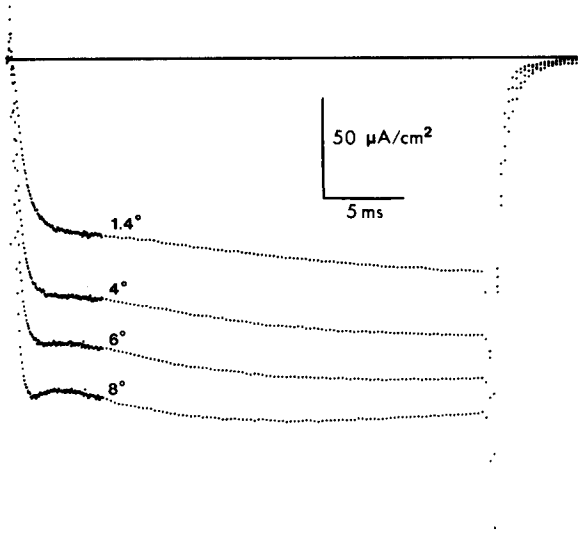

FIGURE 2. Na currents recorded from a pronase-treated fiber during 30-ms voltage-clamp steps to +30 mV at each of the indicated temperatures. Temperature was changed in the following sequence: 1.4, 4, 6, 8°C. The Q_{10} of current amplitude measured near the end of the pulse was 2.30. The biphasic activation pattern is apparent in all traces. Axon AU200A. Holding potential was −80 mV. 1/4 Na//200 TMA.

values at $t = 0$ are the control Na currents recorded in the absence of a prepulse. With 200 mM tetramethylammonium (TMA) as the internal solution (open circles in Fig. 4), Na current recovers to control levels within 5 ms after the inactivating prepulse. As the interpulse interval is increased further, the current amplitude increases until at ~20 ms the current is ~45% greater than the control level. The "potentiated" current level then declines as the interpulse interval increases further until at ~500 ms the current is at the control level. In various fibers the amount of potentiation varies from as little as 10% to as much as 45%. Furthermore, the effect increases with time during an experiment; i.e., axons that show little or no potentiation at the beginning of an experiment may develop 30–40% potentiation in 1–3 h. Control and

potentiated Na currents are shown in Fig. 4B. It is noteworthy that only the peak current is increased after the prepulse. The two currents approach the same steady-state level at the end of the voltage-clamp step.

With 275 mM KFG perfusing the axon (after the K channels have functionally disappeared; see Almers and Armstrong, 1980) inactivation appears more complete (Fig. 4A). This was also evidenced by a larger ratio of peak to steady state Na current in 275 KFG than in 200 TMA. However, there is nearly as much potentiation of the Na current in 275 KFG (43%) as in 200

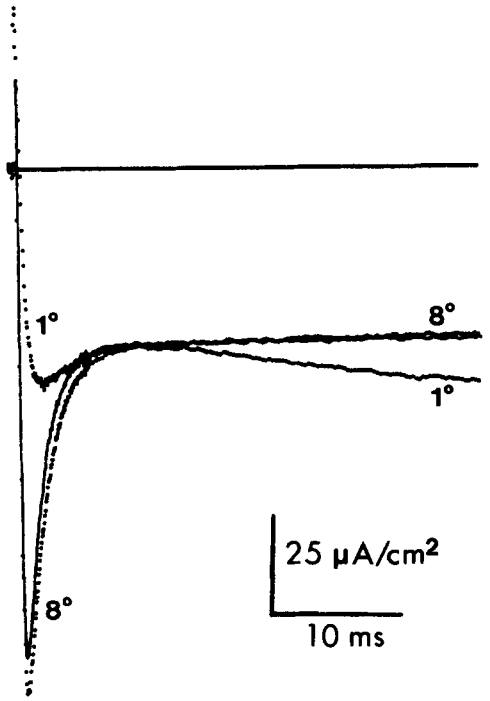

FIGURE 3. Slow activation phase in nonpronased fiber. These currents were generated by voltage-clamp steps to +60 mV at each of the indicated temperatures. Temperature was changed from 8 to 1 to 8°C (the solid trace was recorded last). The slow activation phase only appears in the trace recorded at 1°C, which indicates that its appearance was a reversible effect of temperature. Axon AU119A. The holding potential was −80 mV. 1/5 Na//200 TMA.

TMA (Fig. 4A). In addition, potentiation occurs both with a cesium flouride solution perfusing the fiber and with outward Na currents obtained by adding 20 mM NaF to the 200 TMA solution. Thus the potentiation effect apparently does not depend on the composition of the solution.

The additional peak conductance activated by the large positive prepulse has roughly the same voltage dependence as normal peak Na conductance. An experiment demonstrating this result is summarized in Fig. 5. Na currents were generated by voltage-clamp steps to various potentials, either in the

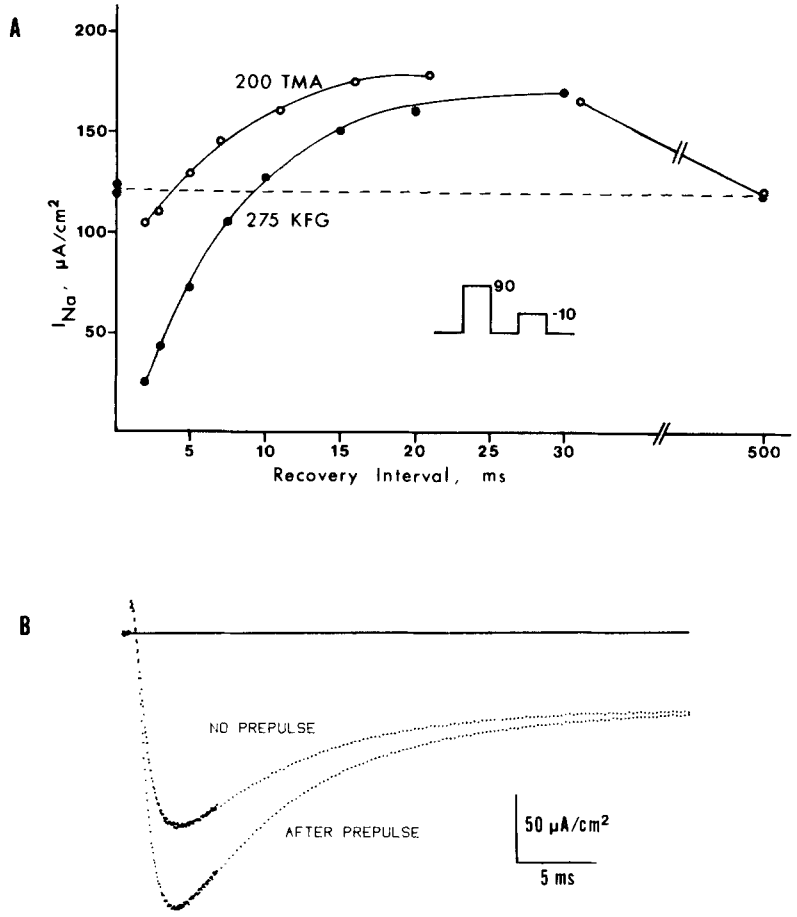

FIGURE 4. Recovery from inactivation illustrating the potentiation effect. The pulse protocol for this experiment is shown in the inset of A. (A) Peak current amplitude generated by the pulse to −10 mV is plotted as a function of the interval between pulses. The points lying on the ordinate represent control currents recorded in the absence of a prepulse and the dashed line also represents the control level. With either 200 TMA or 275 KFG perfusing the axon, current amplitude is higher than the control level for an appropriate spacing of pulses. Axon AU119A. The temperature was 1°C and the holding potential was −80 mV. (B) Sample Na currents from the same experiment shown in part A. Only the peak current is potentiated by the prepulse; the two currents approach the same steady state level. The test pulse was to +20 mV, the prepulse was to +80 mV, and the recovery interval was 15 ms. 1/5 Na//200 TMA.

presence or absence of a 15-ms prepulse to +100 mV. In Fig. 5A are plotted the peak current-voltage relationships found in the absence (filled circles) or presence (open circles) of a prepulse. The difference between these two curves (stars) therefore reflects the additional current activated by the prepulse. The

voltage dependence of the extra conductance is shown in Fig. 5B. Conductance was calculated by dividing the current by the driving force, using a Na equilibrium potential of 90 mV (which was obtained from the *I-V* plots of Fig. 5A). It is apparent that the extra conductance has similar voltage dependence to the normal peak conductance.

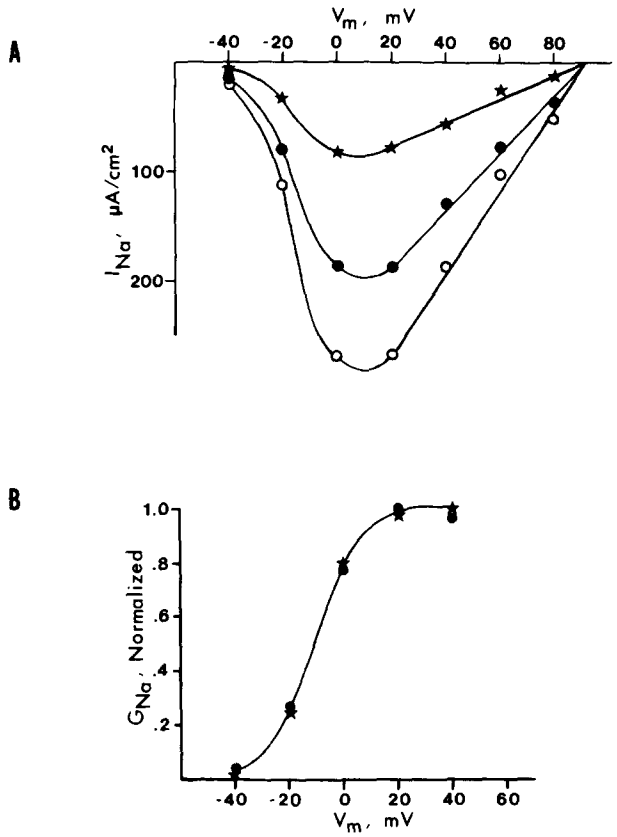

FIGURE 5. (A) Peak current-voltage relationships. The filled circles plot the current-voltage relationship in the absence of a prepulse and the open circles represent current after a prepulse. The stars plot the difference between the two curves and therefore represent the extra current induced by the prepulse. The shape and position of the curves appears relatively constant. Axon AU209A. Prepulses were to +100 mV for 15 ms. Temperature 5°C. The holding potential was −80 mV. 1/4 Na//200 TMA. (B) Conductance-voltage relationships for peak Na conductance (filled circles) and for the extra conductance induced by the prepulse (stars). Conductance was calculated by dividing the current (which was plotted in A) by the driving force, assuming a Na equilibrium potential of 90 mV (i.e., the intersection of the *I-V* curves in A with the voltage axis). The extra conductance induced by the prepulse clearly has the same voltage dependence as normal peak conductance.

Factors Influencing Potentiation

The voltage level of the prepulse determines the degree of potentiation of the current that is generated by the second pulse, as illustrated in Fig. 6. Potentiation above the current level seen in the absence of a prepulse is plotted as a function of prepulse voltage (squares in Fig. 6). The prepulse duration

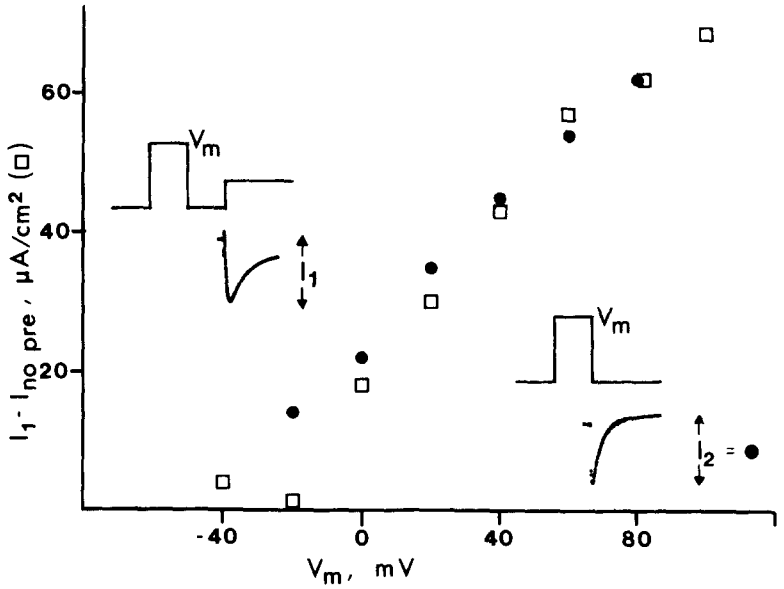

FIGURE 6. Voltage dependence of potentiation and steady state conductance. The pulse protocol in the inset to the upper left was used to determine the voltage dependence of potentiation. The test pulse was to 0 mV and interpulse interval was 25 ms. The open squares plot the extra peak current induced by the prepulse as a function of prepulse voltage. Axon AU149A. 1/4 Na//200 TMA. The level of steady state conductance was estimated from the height of tail currents induced by repolarization from 20-ms steps to the indicated voltages (see inset at lower right). Tail current amplitudes were normalized so that tail height and potentiation values were equal at +80 mV. Tails were recorded from axon SE130Y. The holding potential was −80 mV. 1/4 Na//200 TMA + 20 NaF.

was fixed at 30 ms and the interpulse interval was 25 ms. The potentiating effect of the prepulse becomes evident at 0 mV and increases as the prepulse is made more positive. For comparison, the voltage dependence of steady state sodium conductance is also plotted in Fig. 6. The steady state conductance curve was determined by measuring the amplitude of the Na current tails generated upon repolarization to the holding potential after a 20-ms step to the indicated voltage. Tail current amplitudes have been normalized so that the two curves plotted in Fig. 6A coincide at 80 mV. The close correlation in voltage dependence of the potentiation effect and steady state Na conductance

suggests that the amount of potentiation is related in some way to the amount of steady state conductance activated during the prepulse. We will develop this point more fully in the discussion.

The degree of potentiation is also a function of the temperature. As the temperature was lowered the amount of potentiation (measured as the percentage increase in peak Na current) became larger. This is illustrated by the Na current pairs shown in Fig. 7. In each pair the smaller current was

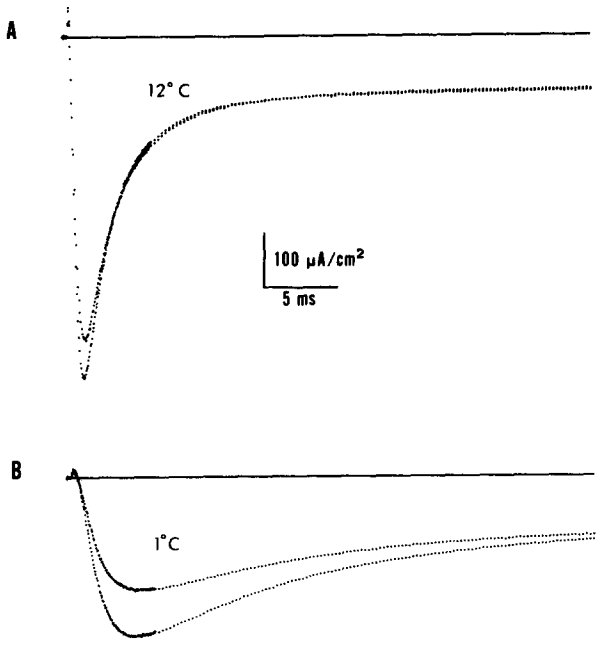

FIGURE 7. The effect of temperature on potentiation. All currents were generated by voltage-clamp steps to 0 mV. In both A and B the smaller current was recorded in the absence of a prepulse and the larger current followed a prepulse to +100 mV. The relative increase in current following the prepulse is clearly greater at 1°C than at 12°C. Axon AU149A. 1/4 Na//200 TMA.

generated in the absence of a prepulse and the larger current was evoked after a prepulse to 100 mV. At 1°C (Fig. 7B) potentiation was 40%, whereas at 12°C (Fig. 7A) potentiation was only 12%.

As suggested above, one possible explanation of the results presented thus far involves the idea that there is a population of slowly activating Na channels that does not inactivate and therefore contributes to the steady state Na conductance. Because the potentiation effect and steady state conductance have similar voltage dependencies (Fig. 6), one might suppose that the prepulse effectively speeds the activation kinetics of some of the "sleepy" channels for several hundred milliseconds so that they contribute to the peak Na current generated by a subsequent test pulse. If this were the case, the

slow activation phase of Na currents (cf. Figs. 2 and 3) should be reduced or abolished by positive prepulses. This in fact occurs as shown in Fig. 8. The current pair shown in Fig. 8A was taken from a pronased fiber and the pair in Fig. 8B is from a nonpronased fiber. In both cases, the effect of the prepulse

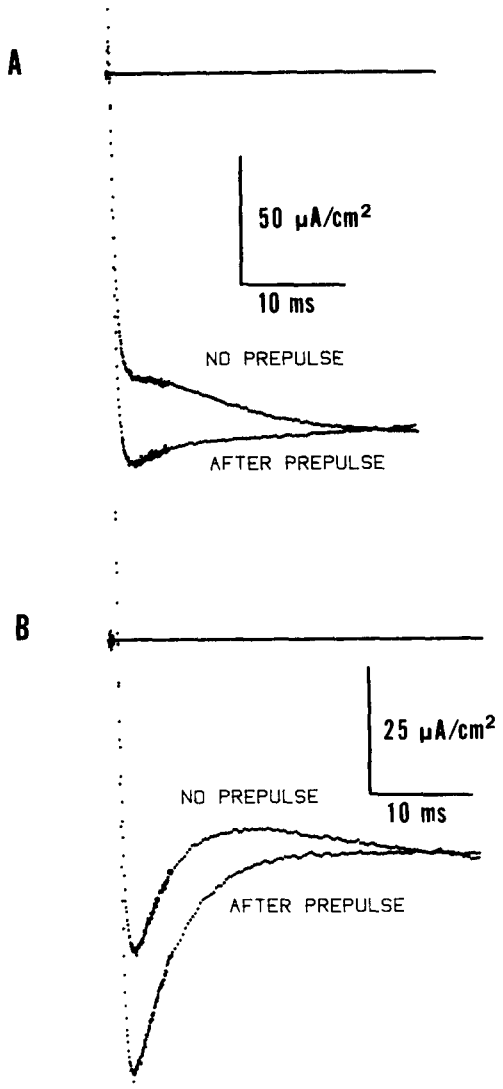

FIGURE 8. Elimination of the slow activation phase by potentiating prepulses. (A) Currents generated by steps to +30 mV in a pronase-treated fiber. The prepulse was to +100 mV for 25 ms. Axon AU200A. Temperature, 4°C. 1/4 Na//200 TMA. (B) Currents generated by steps to +60 mV in a nonpronased fiber. Prepulse was to +100 mV for 30 ms. Axon AU149A. Temperature, 1°C. 1/4 Na//200 TMA. In both cases the prepulse increased the early current, eliminated the slow activation phase, and had relatively little effect on the steady state current magnitude.

is to increase the early, peak Na current and to abolish the slow activation phase. The final steady state current level is unaffected by the prepulse. This result is consistent with the hypothesis that the activation kinetics of the "sleepy" channels are sped up by the prepulse. It is assumed that these channels do not inactivate, so that the steady state current level would be the same if the sleepy channels open slowly (in the absence of a prepulse) or rapidly (after a large prepulse).

DISCUSSION

The major findings presented in this paper can be summarized as follows. (*a*) Steady state sodium currents are relatively unaffected by changes in temperature, whereas peak Na currents decrease substantially as the temperature is lowered. (*b*) Na currents generated at positive voltages and low temperatures sometimes exhibit both fast and slow activation phases. The currents activate, partially inactivate, and then increase slowly to an apparently sustained level. (*c*) Peak Na current amplitude can sometimes be potentiated by delivering large positive prepulses, and the potentiation effect is more pronounced at low temperatures. The amount of potentiation seems to be correlated with the amount of steady state conductance activated during the prepulse.

We have considered many possible explanations of these results. The differential effect of temperature on peak and steady state current could result from an altered equilibrium between the open and inactivated states, such that the open state is favored at low temperature. A high Q_{10} for single-channel conductance would be required to explain the decrease in peak current as the temperature falls, but the steady state current would remain unchanged because of the larger number of channels that are not inactivated. Following this explanation one can estimate the enthalpy change associated with the transition from the open to the inactivated state from the change in apparent equilibrium constant. This enthalpy difference predicts a Q_{10} of the rate constant of the open to inactivated transition which is much larger than we observe experimentally. Therefore, this explanation seems unlikely.

A second possibility is that closed channels can reach the inactivated state by two pathways, only one of which is through the open state, and that the two paths have different Q_{10}'s. For example, in the Armstrong and Bezanilla (1977) kinetic model of the Na channel, the inactivated state (X_1Z) can be reached either through the open state (X_1^*) or, bypassing the open state, through X_2Z. On the basis of this model one might explain the differential effect of temperature on peak and steady state Na current under the assumption that the Q_{10} of the transition from X_2 to X_1^* is greater than the Q_{10} of the transition from X_2 to X_2Z. As the temperature is lowered, a larger fraction of channels would pass through X_2Z instead of X_1^* upon depolarization, resulting in smaller peak current. For a Q_{10} of single-channel conductance near 1, steady state current would be temperature independent because it is due to an equilibrium between the open and inactivated states of the channel. This model predicts that after pronase treatment (which eliminates the path from X_2 to X_2Z) Na current amplitude should be temperature independent, but

this was not found experimentally, which led us to reject the model and any similar model that explains the temperature effect as resulting from different pathways of inactivation at different temperatures.

It has been hypothesized by Chandler and Meves (1970*a*) that steady state Na current is generated by a second conducting state of the channel, which they called h_2. On the basis of this model, a third interpretation of the differential temperature effect could be that conductance in the h_2 state is temperature independent, whereas peak conductance is highly temperature dependent. Thus if the same number of Na channels operate at all temperatures, peak current would decrease and steady state current would remain the same. We cannot completely reject this hypothesis, but we dislike it for the following reasons. First, steady state conductance often has a Q_{10} of <1 (Fig. 1), which the hypothesis cannot explain. Second, potentiation by positive prepulses is not easily incorporated into this scheme.

The final model we considered, which is most consistent with our results, hypothesizes that there are two forms, or subpopulations, of the Na channel. One subpopulation has rapid activation kinetics and, perhaps, completely inactivates. This is the classic Na channel first described by Hodgkin and Huxley (1952). The second subpopulation, the sleepy Na channels, is assumed to have activation kinetics that are approximately one order of magnitude slower than the fast channels. In addition, we assume that this subpopulation either does not inactivate or inactivates very slowly, so that it generates the steady state current. The time course of sleepy channel activation is indicated by the slow Na current increase seen in Figs. 2 and 3.

We have modeled Na channel currents on the basis of this two-channel hypothesis and the proposed state diagrams are shown in Fig. 9. The fast channel scheme is simply the sequential model of Bezanilla and Armstrong (1977) and Armstrong and Gilly (1979). We assume here that the rate constant for the transition from the inactivated state (X_1Z) to the open state X_1^* is zero; i.e., these channels completely inactivate. However, the existence of a small number of noninactivating fast channels would not be inconsistent with our results. A theoretical current through these fast channels is shown at the bottom of Fig. 9, and the state diagram for the sleepy channels is shown in the middle of the figure. States X_6 through X_1^* are identical to the normal channels. The differences in state diagrams from normal and sleepy channels are: (*a*) a sleepy state (X_s) which is the most likely resting state of the sleepy channels; upon depolarization this state equilibrates very slowly with X_1^*, i.e., α_s and β_s are small; and (*b*) inactivation is very slow or nonexistent; i.e., κ_s is small or zero. Therefore, during a 36-ms voltage-clamp step there is insignificant inactivation of sleepy channels as shown by the theoretical current at the bottom of Fig. 9. The total Na current that one records would then be the sum of the currents generated by these two subpopulations of channels, and is given by the solid trace at the bottom of Fig. 9. Quantitative fits of this model to experimental traces are given below.

In some ways the two-channel model resembles the "precursor-partial dissociation" model proposed by Wu et al. (1980) to explain the action of

deoxycholate (DOC) on squid axon sodium currents. In their model, it is assumed that DOC binds to the closed state of the channel and that upon depolarization DOC must partially dissociate from the channel before activation can occur. In our model we chose not to place the sleepy state (X_s) at the beginning of the activation sequence (i.e., in equilibrium with X_6) because sleepy channel conductance, which is assumed to generate the steady state

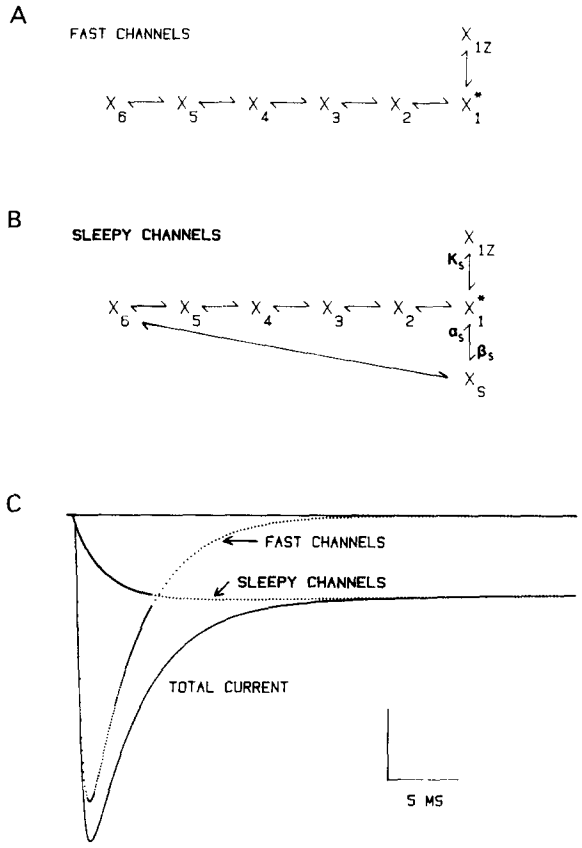

FIGURE 9. State diagrams of the two types of Na channels. Only those states that would be significantly populated during a depolarization are shown (states relating to recovery from inactivation are not shown). See text for other details.

current, has a voltage dependence that is different from that of peak conductance (cf. Figs. 5 and 6), which is difficult to fit with this model. If states X_6 through X_1* are the same for both channel types and if X_s were simply assumed to equilibrate slowly with X_6, fast channel and sleepy channel conductance would have similar voltage dependencies.

The two-channel model can explain the potentiating effect of positive prepulses in the following way. After a sufficiently long depolarization many

or most sleepy channels will be "awakened" and in state X_1*. Upon repolarization, some fraction of these channels can close through state X_2 to X_6, and in response to a subsequent depolarization they can reopen by the same pathway (X_6 to X_1*). Because the rate constants for the transitions from X_6 to X_1* are much faster than for a transition from X_s to X_1*, these awakened sleepy channels activate more rapidly, thereby contributing to peak Na current. This is the basis for potentiation. After repolarization the awakened channels slowly go back to sleep; i.e., they undergo a transition from X_6 to X_s, which explains the decay of the potentiation effect after the prepulse. According to this two-channel model, the sleepy ones in state X_1* are responsible for steady state conductance and, since they can close to X_6, for prepulse potentiation. Therefore, the correlation between steady state conductance and the extra current induced by the prepulse, which was shown in Fig. 6, is consistent with the model.

The potentiation effect increases as the temperature decreases, and we therefore hypothesize that normal Na channels are converted to sleepy ones by cooling. Channel conversion might occur as a result of a phase transition in the lipid phase of the membrane or possibly in the channel protein itself. Kumamoto et al. (1971) indicated that a change in activation energy of a biological reaction accompanies a phase transition of the system under study. Thus the occurrence of the transition can be demonstrated as a change in slope or a break in an Arrhenius plot. Schwarz (1979) showed that Arrhenius plots of the Hodgkin and Huxley (1952) parameters τ_m and τ_h calculated from frog skeletal muscle Na currents exhibited changes in slope at a temperature of 5–8°C, and he concluded that either the channel protein or the surrounding lipid has undergone a phase change. It is conceivable that a phase transition might alter the interaction between the Na channel protein and membrane lipid so as to cause conversion of normal, fast Na channels to sleepy channels.

We have calculated Na currents from the model shown in Fig. 9 in a manner similar to that described by Armstrong and Gilly (1979). For these calculations, it was assumed that all fast channels start in state X_6 and all slow channels start in state X_s at the holding potential (−80 mV). In addition, both channel types were assumed to have the same reversal potential and single-channel conductance. The rate constants for all steps to the left of X_2 were assumed to be the same. The equilibrium constants for voltage-dependent transitions were assumed to be exponential functions of voltage (see Eqs. 2 and 3 in Armstrong and Gilly [1979]).

The Na currents illustrated in Fig. 10 (smooth traces) were calculated using the parameter values shown in Table III and are plotted together with actual data (dotted traces). It is clear from this figure that the two-channel model accurately fits Na currents and also accurately reproduces the different voltage dependence and temperature dependence of peak and steady state Na conductance. It was assumed that the fraction of fast channels was 65% at 8°C (Fig. 10A) and 49.5% at 1°C (Fig. 10B). Thus the model indicates that as the temperature decreases, steady state conductance remains approximately con-

stant because the decrease in single-channel conductance is offset by the larger number of sleepy channels conducting in the steady state.

The Q_{10}'s of the model parameters can readily be calculated from the data in Table III and these Q_{10} values from several experiments are shown in Table IV. It is interesting that the Q_{10} of maximum sodium conductance is ~1.8, which is not far from the Q_{10} of diffusion in free solution. The fact that the Q_{10}

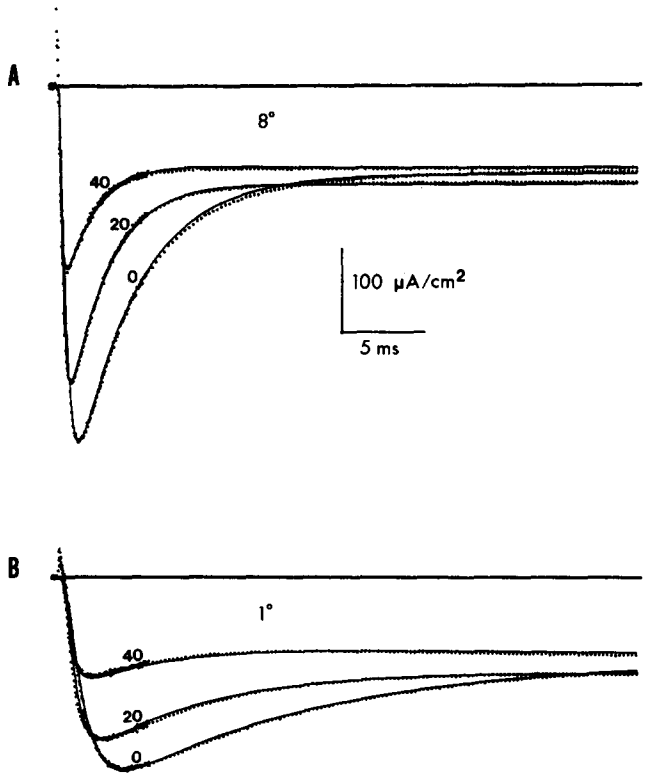

FIGURE 10. Comparison of experimental Na currents (dotted traces) with currents calculated from the model of Fig. 9 (solid traces). Parameter values are given in Table III. Experimental currents were recorded at each of the indicated voltages at either 8°C (A) or 1°C (B). Axon AU109B.

for peak Na current reported in this paper and by Kimura and Meves (1979) is significantly larger than 1.8 could be partially due to the transformation of fast channels to sleepy channels by cooling. This transformation would result in fewer channels conducting at the peak of the Na current at the lower temperature, which would effectively increase the measured Q_{10}.

The effects produced by the detergent DOC as reported by Wu et al. (1980) were similar in many respects to effects produced by cooling. These authors

reported that micromolar concentrations of DOC decreased peak Na currents and increased steady state Na currents. Furthermore, after DOC application Na currents took on a pattern of activation and partial inactivation followed by a secondary activation phase, which is qualitatively the same pattern that we often see in normal fibers at low temperatures and positive voltages (Fig. 3). Thus, DOC induces a slowly activating, noninactivating Na conductance and because DOC alters membrane protein-lipid interactions it is possible that the detergent and cooling alter the Na channel in an analogous manner.

TABLE III

MODEL PARAMETERS FOR FIG. 10

V_m	Temperature	α_1	α_{2-5}	β_1	β_{2-5}	κ	α_s	β_s	CSF*
	°C								
0	8	3.6	16	0.326	4.82	0.3	0.096	0.174	29,810
20	8	5.0	20	0.092	2.7	0.37	0.14	0.122	21,388
40	8	6.4	21	0.024	1.3	0.43	0.192	0.06	12,400
0	1	1.3	6.72	0.118	2.0	0.096	0.0372	0.068	19,780
20	1	1.8	8.4	0.033	1.14	0.12	0.052	0.045	14,600
40	1	2.6	8.8	0.0096	0.548	0.134	0.07	0.026	8,530
Q_{10}		4.1	3.5			5.1	4.1		1.7

* CSF is a current scaling factor, which was multiplied by X_1* to obtain current magnitude, and is equal to maximum sodium conductance times (V-V_{Na}).

All rate constants are in units of ms^{-1}. The initial conditions for the 8°C records was $X_6 = 0.65$ and $X_s = 0.35$ and for the 1°C records was $X_6 = 0.495$ and $X_s = 0.505$. K_s was assumed to be zero.

TABLE IV

Q_{10}'S OF VARIOUS PARAMETERS

Experiment	α_1	α_{2-5}	α_s	κ	$\bar{g}_{Na}$
AU109B	4.1	3.5	4.1	5.1	1.7
AU119A	3.3	3.0	4.4	4.3	1.7
AU149A	3.7	3.7	3.6	4.5	1.8
AU229C	4.1	4.0	3.9	4.4	1.9
SE100Z	2.7	2.8	4.1	3.9	1.7
Mean ± SD	3.6±0.59	3.4±0.49	4.0±0.29	4.4±0.43	1.8±0.09

It has recently been reported that venoms from the scorpions *Leiurus quinquestriatus* and *Centruroides sculpturatus* also induce Na currents that activate biphasically (Gillespie and Meves, 1980). It is conceivable that these toxins are also transforming normal channels into slowly activating sleepy channels. It would be extremely advantageous to have a reagent that preferentially blocks either peak or steady state Na conductance. Such a reagent would present pharmacological evidence for two channel types. Because *n*-octanol is a more potent blocker of steady state conductance than of peak conductance (Oxford and Swenson, 1979), it may be the required pharmacological agent. We are planning experiments to investigate this possibility.

Several obvious questions remain that cannot be answered at the present time. First, most of our experiments have been done in August and although we have not done a careful study there may be some seasonal variability in the potentiation phenomenon. Such variability might conceivably be caused by a change in the lipid composition of the membrane as the animal adapts to changes in water temperature. In addition, the fact that potentiation usually becomes more prominent with time during an experiment might be caused by an alteration of the membrane lipids during voltage clamping. One final question concerns how much of the steady state sodium current is from sleepy channels. Although we assumed that there was no steady state conductance associated with normal channels, our data could be fit equally well if some normal channels had a noninactivating component of current. Answers to these questions must await further investigation.

Received for publication 20 April 1980 and in revised form 8 September 1981.

REFERENCES

ALMERS, W., and C. M. ARMSTRONG. 1980. Survival of K^+ permeability and gating currents in squid axons perfused with K^+-free media. *J. Gen. Physiol.* **75**:61–78.

ARMSTRONG, C. M., and F. BEZANILLA. 1974. Charge movement associated with the opening and closing of the activation gates of the Na channels. *J. Gen. Physiol.* **63**:533–552.

ARMSTRONG, C. M., and F. BEZANILLA. 1977. Inactivation of the sodium channel. II. Gating current experiments. *J. Gen. Physiol.* **70**:567–590.

ARMSTRONG, C. M., F. BEZANILLA, and E. ROJAS. 1973. Destruction of sodium conductance inactivation in squid axons perfused with Pronase. *J. Gen. Physiol.* **62**:375–391.

ARMSTRONG, C. M., and W. F. GILLY. 1979. Fast and slow steps in the activation of sodium channels. *J. Gen. Physiol.* **74**:691–711.

BEZANILLA, F., and C. M. ARMSTRONG. 1977. Inactivation of the sodium channel. I. Sodium current experiments. *J. Gen. Physiol.* **70**:549–566.

BEZANILLA, F., and R. E. TAYLOR. 1978. Temperature effects on gating currents in the squid giant axon. *Biophys. J.* **23**:479–484.

CHANDLER, W. K., and H. MEVES. 1970*a*. Evidence for two types of sodium conductance in axons perfused with sodium fluoride solution. *J. Physiol. (Lond.)*. **211**:653–678.

CHANDLER, W. K., and H. MEVES. 1970*b*. Rate constants associated with changes in sodium conductance in axons perfused with sodium fluoride. *J. Physiol. (Lond.)*. **211**:679–705.

CHAPMAN, D. 1975. Phase transitions and fluidity characteristics of lipids and cell membranes. *Q. Rev. Biophys.* **8**:185–235.

CHIU, S. Y., H. E. MROSE, and J. M. RITCHIE. 1979. Anomalous temperature dependence of the sodium conductance in rabbit nerve compared with frog nerve. *Nature (Lond.)*. **279**:327–328.

FRANKENHAEUSER, B., and L. E. MOORE. 1963. The effect of temperature on the sodium and potassium permeability changes in myelinated nerve fibers of Xenopus Laevis. *J. Physiol. (Lond.)*. **169**:431–437.

GILLESPIE, J. I., and H. MEVES. 1980. The effect of scorpion venoms on the sodium currents of the squid giant axon. *J. Physiol. (Lond.)*. **308**:479–499.

HODGKIN, A. L., and A. F. HUXLEY. 1952. A quantitative description of membrane current and its application to conduction and excitation in nerve. *J. Physiol. (Lond.)*. **117**:500–544.

KIMURA, J. E., and H. MEVES. 1979. The effect of temperature on the asymmetrical charge movement in squid giant axons. *J. Physiol. (Lond.)*. **289:**479–500.

KUMAMOTO, J., J. K. RAISON, and J. M. LYONS. 1971. Temperature "breaks" in Arrhenius plots: a thermodynamic consequence of a phase change. *J. Theor. Biol.* **31:**47–51.

LLINAS, R., and M. SUGIMORI. 1980. Electrophysiological properties of in vitro Purkinje cell somata in mammalian cerebellar slices. *J. Physiol. (Lond.)*. **305:**171–195.

MATTESON, D. R., and C. M. ARMSTRONG. 1980*a*. A population of slowly activating Na channels at low temperatures. *Biophys. J.* **33:**280*a*.

MATTESON, D. R., and C. M. ARMSTRONG. 1980*b*. Temperature effects on peak and steady state Na currents in squid giant axons. *Biol. Bull.* **159:**488 (Abstr.).

OXFORD, G. S., and R. P. SWENSON. 1979. *n*-Alkanols potentiate sodium channel inactivation in squid giant axons. *Biophys. J.* **26:**585–590.

SCHAUF, C. L. 1973. Temperature dependence of the ionic current kinetics of *Myxicola* giant axons. *J. Physiol. (Lond.)*. **235:**197–205.

SCHWARZ, W. 1979. Temperature experiments on nerve and muscle membranes of frogs. Indications for a phase transition. *Pfluegers Arch. Eur. J. Physiol.* **382:**27–34.

WU, C. H., P. J. SIDES, and T. NARAHASHI. 1980. Interaction of deoxycholate with the sodium channel of squid axon membranes. *J. Gen. Physiol.* **76:**355–379.